AD-759 543

HIGH ALTITUDE PLASMA EFFECTS. PARAMETRIC EXCITATION BY AN ELECTROMAGNETIC PUMP IN A LARGE LABORATORY PLASMA (QUIPS: QUIESCENT PLASMA STUDIES):FIRST RESULTS

Donald Arnush, et al

TRW Systems Group

Prepared for:

Rome Air Development Center
Advanced Research Projects Agency

February 1973

DISTRIBUTED BY:

NTIS

National Technical Information Service
U. S. DEPARTMENT OF COMMERCE
5285 Port Royal Road, Springfield Va. 22151

AD 759543

RADC-TR-73-128
Technical REport
February 1973

HIGH ALTITUDE PLASMA EFFECTS

TRW Systems Group

Sponsored by
Defense Advanced Research Projects Agency
ARPA Order No. 1423

D D C
RECEIVED
MAY 22 1973
C

Approved for public release;
distribution unlimited.

The views and conclusions contained in this document are those of the authors and should not be interpreted as necessarily representing the official policies, either expressed or implied, of the Defense Advanced Research Projects Agency or the U. S. Government.

Reproduced by
NATIONAL TECHNICAL
INFORMATION SERVICE
U S Department of Commerce
Springfield VA 22151

Rome Air Development Center
Air Force Systems Command
Griffiss Air Force Base, New York

41
R

UNCLASSIFIED
Security Classification

DOCUMENT CONTROL DATA - R & D

(Security classification of title, body of abstract and indexing annotation must be entered when the overall report is classified)

1. ORIGINATING ACTIVITY (Corporate author)
TRW Systems Group

2a. REPORT SECURITY CLASSIFICATION
UNCLASSIFIED

2b. GROUP

3. REPORT TITLE
HIGH ALTITUDE PLASMA EFFECTS

4. DESCRIPTIVE NOTES (Type of report and inclusive dates)
Interim Report (21 July 1972-31 January 1973)

5. AUTHOR(S) (First name, middle initial, last name)
Donald Arnush, Charles F. Kennel
Burton D. Fried, Alfred Y. Wong

6. REPORT DATE
February 1973

7a. TOTAL NO. OF PAGES
30

7b. NO. OF REFS
0

8a. CONTRACT OR GRANT NO.
F30602-72-C-0304

b. PROJECT NO.
ARPA Order No. 1423

c.

d.

9a. ORIGINATOR'S REPORT NUMBER(S)
21961-6005-RU-00

9b. OTHER REPORT NO(S) (Any other numbers that may be assigned this report)
RADC-TR-73-128

10. DISTRIBUTION STATEMENT
Approved for public release; distribution unlimited.

11. SUPPLEMENTARY NOTES
MONITORED BY:
RADC/OCSE
GAFB, NY 13441

12. SPONSORING MILITARY ACTIVITY
Advanced Research Projects Agency
1400 Wilson Blvd
Arlington, VA 22209

13. ABSTRACT

A series of experiments are being carried out in the TRW large volume plasma facility, the QUIPS (Quiescent Plasma Studies) device. The purpose of the experiments is to study those parametric instabilities which are excited when high power microwaves propagate into a plasma cutoff region. The plasma instabilities have been observed with probes; in later experiments, Thompson radar scattering diagnostics will also be used. A variety of nonlinear effects which are consistent with the standard linear theory of parametric instabilities were observed, as well as other phenomena which are still the subject of theoretical study. Since these experiments have been running only three months and are still in progress, many of the results must be considered preliminary.

The device, the properties of the quiescent plasma, and the wave modes are discussed. The experimental results are grouped into the following topics:

1. Parametric excitation of high frequency sidebands near the pump frequency;
2. Excitation of low frequency oscillations;
3. Propagation of ion acoustic waves in the presence of an electromagnetic wave pump; and
4. Mode coupling of electron plasma waves and ion acoustic waves by an electromagnetic wave pump.

Future experiments will include the use of specially designed probes, now under construction, and of 4mm and 8mm scattering diagnostics, which will be installed.

DD FORM 1 NOV 65 1473

UNCLASSIFIED
Security Classification

14 KEY WORDS	LINK A ROLE	LINK A WT	LINK B ROLE	LINK B WT	LINK C ROLE	LINK C WT
Plasma						
Ionospheric Simulator						
Parametric Instability						
Probe Measurements						

RADC-TR-73-128
Technical REport
February 1973

HIGH ALTITUDE PLASMA EFFECTS

TRW Systems Group

Sponsored by
Defense Advanced Research Projects Agency
ARPA Order No. 1423

Approved for public release;
distribution unlimited.

The views and conclusions contained in this document are those of the authors and should not be interpreted as necessarily representing the official policies, either expressed or implied, of the Defense Advanced Research Projects Agency or the U. S. Government.

Rome Air Development Center
Air Force Systems Commond
Griffiss Air Force Bose, New York

HIGH ALTITUDE PLASMA EFFECTS

Donald Arnush
Burton D. Fried
Charles F. Kennel
Reiner L. Stenzel
Alfred Y. Wong

Contractor: TRW Systems Group
Contract Number: F30602-72-C-0304
Effective Date of Contract: 28 February 1972
Contract Expiration Date: 15 September 1973
Amount of Contract: $129,392.00
Program Code Number: 2E20

Principal Investigator: B. D. Fried
Phone: 213 536-2266

Project Engineer: Vincent J. Coyne
Phone: 315 330-3107

Contract Engineer: T. A. DeMesme
Phone: 315 330-2387

Approved for public release;
distribution unlimited.

This research was supported by the Defense Advanced Research Projects Agency of the Department of Defense and was monitored by T.A. DeMesme RADC (OCSE), GAFB, NY 13441 under Contract F30602-72-C-0304.

TRW #21961-6005-RU-00

Parametric Excitation by an Electromagnetic Pump in a Large Laboratory Plasma (QUIPS: Quiescent Plasma Studies): First Results.

HIGH ALTITUDE PLASMA EFFECTS

Interim Report
26 July 1972 - 30 January 1973

by

D. Arnush
B.D. Fried
C.F. Kennel
R.L. Stenzel
A.Y. Wong

TRW Systems Group

This research was supported by the Advanced Research Projects Agency of the Department of Defense and was monitored by Vince Coyne under Contract No. F30602-72-C-0304.

PUBLICATION REVIEW

This technical report has been reviewed and is approved.

RADC Project Engineer

RADC Contract Engineer

SUMMARY

We report experiments carried out in the TRW large volume plasma facility, the QUIPS (Quiescent Plasma Studies) device. The purpose of these experiments is to study parametric instabilities which are excited when high power microwaves propagate into a plasma cutoff region. The plasma instabilities have been observed with probes; in later experiments Thompson radar scattering diagnostics will also be used. We have observed a variety of nonlinear effects in this region which are consistent with the standard linear theory of parametric instabilities, as well as other phenomena which are still the subject of theoretical study. The experiment, which has been running now for about three months, is still in progress, so many of our results must still be considered as preliminary. In some experiments ambiguities in interpretation were encountered due to interactions between the pump and plasma waves, and the probes. These will hopefully be resolved by the use of specially designed probes now under construction, and of 4 mm and 8 mm scattering diagnostics which will soon be installed.

I. PLASMA DEVICE AND PLASMA PARAMETERS

The plasma device is 2m in diameter and 4m in length (see Figure 1). Plasma is produced by a dc discharge in argon at about 1μ pressure. Two rings of tungsten filaments, biased about 40-60 volts below the chamber wall, act as cathode and the chamber wall as anode. The chamber wall is lined with 10,000 permanent magnets so as to reduce the plasma losses. The filament rings are located near one end of the chamber, which produces the desired axial density gradient. Electromagnetic waves are launched from a dipole at the focus of the parabolic antenna (radius 40 cm) and propagated into the density gradient along the axis of the device.

Plasma diagnostics and wave diagnostics are performed with two radial probes and one axial probe, all movable with automatic probe-drive systems. With the radial probes we investigate wave propagation parallel to the electric field of the electromagnetic wave, which is the direction where the strongest interaction occurs. However, the shaft of this probe is parallel to the pump electric field, which perturbs the electromagnetic field pattern as the probe moves. The axial probe is in this respect better arranged because it has a minimum scattering cross section for electromagnetic waves, the shaft being perpendicular to the pump electric field. Three different types of probes are employed: 1) A magnetic loop antenna which picks up only the electromagnetic waves; 2) a shielded triple grid which launches and detects plasma waves; and 3) various coaxial Langmuir probes which are used to determine basic plasma parameters and to detect plasma waves and electromagnetic waves.

The basic plasma parameters are summarized in Table 1. At high pressures, typically 1.3 microns of argon, we obtain plasma densities around 5×10^{10} cm^{-3} which corresponds to a plasma frequency of about 2000 megacycles. The electron temperature is about 1.6 electron volts. The low frequency noise, when measured from the electron saturation current fluctuations, and integrated over the entire range of ion acoustic waves up to the ion plasma frequency, corresponds to a $\delta n/n$ of about 1%. There is high frequency noise around the electron plasma frequency with bandwidth of about 200 megacycles,

presumably due to beam plasma instabilities caused by the fast primary electrons from the filaments. For the above parameters the density gradient scale length is about 100 centimeters in the axial direction, while the density is much more uniform in the radial direction with a scale length of about 500 cm or longer. At low pressures the plasma properties change drastically. While the primary electron density stays constant for a given discharge voltage and current, the plasma density decreases because the neutral density decreases. This can be seen on the Langmuir traces in Fig. 2. The upper Langmuir probe trace is taken at high pressures. The plasma potential and floating potential are properly separated by a few kTe. In the lower trace the pressure has been lowered by 3 orders of magnitude. The electron density drops significantly (note the change in the current scale), and the primary electrons become easily visible. Taking the second derivative of the Langmuir probe trace yields the electron speed distribution function. One can see a large hump of electrons around -50 volts (the primary electrons) and a second hump near the plasma potential (the plasma electrons with T_e of about 4 electron volts). At low pressures the relative concentration of hot electrons to cold electrons can become as high as 10%. At high pressures ($P \sim 1$ micron) where parametric effects are being investigated, the primary electrons have little importance since their relative concentration has dropped to about 0.1%.

II. BASIC WAVES

There are three types of waves involved: ion acoustic waves, electron plasma waves (Langmuir waves), and electromagnetic waves. Figure 3 shows measured dispersion and damping of ion acoustic waves launched from a grid. The dispersion, ω vs k, is essentially a straight line with slope or phase velocity $v_{ph} = 1.8 \times 10^5$ cm/sec; this is in good agreement with the $c_s = (T_e/M)^{1/2}$ velocity calculated from electron temperature measurements. The damping (Im k/Re k) is about 6×10^{-2}; we attribute this to collisional damping and also to geometric damping effects, since the launching-grid structure is only 10 to 20 wavelengths in diameter. A typical interferometer trace is shown in Fig. 4 (top picture). The lower traces are taken at lower pressures, where the effects of the primary electrons on the wave dispersion become more pronounced. The primary electrons raise the sound speed to a density-weighted average value between the primary electron energy and the plasma electron temperature. The increased phase velocity is nearer to the thermal velocity of the plasma electrons, resulting in heavier Landau damping. The nonexponential spatial damping may be caused by nonlinear effects due to large amplitude excitation of waves. Note that the frequency in the lower two traces has been lowered to half the value of the upper two traces in order to stay well below the ion plasma frequency.

The propagation of Langmuir waves has been studied in the mode coupling process, to be reported further below. The launching and detecting of launched Langmuir waves requires special shielded triple grids, which are presently being built and installed. Except for the effect of primary electrons, one can expect to find a Bohm-Gross type dispersion relation for these waves.

The propagation of microwaves along the tank axis has been studied with and without plasma. Figure 5 shows the axial amplitude dependence of a microwave signal at 2050 MHz without plasma. The wave pattern is somewhat distorted due to reflections from the end walls and interference patterns in the near zone of the antenna. The electric field strength has been measured

by the small magnetic loop antenna and compared with a calibration field outside of the tank. This calibration field is set up with a standard gain horn antenna with known input power at a known distance from the detector probe. This calibration yields a peak electric field of 70 mV/cm for 1 watt input at the experimental region inside of the plasma device, i.e., the intersection between the radial probe and the axial probe.

When the microwaves are propagated in the presence of the plasma (see Figure. 6) we observe a well-defined cutoff region. The density of this region, as measured from Langmuir probes, gives a plasma frequency in good agreement with the signal frequency. The region of interest lies around the last standing wave peaks of the pump pattern before cutoff. In this region we look for nonlinear coupling between microwaves and plasma waves propagating parallel to the pump electric field. The pump pattern on the propagating side is distorted by reflections from the back wall. This situation will be remedied by the installation of fine wire microwave absorbers on the back wall surrounding the antenna. Motion of radial probes, parallel to the electric field in this region, perturbs the pattern significantly. Typical perturbations of the pump pattern by moving the radial probes are shown in Figure 7. The signal is picked up by the stationary axial probe while the radial probe moves to a position as indicated on the horizontal axis. The various peaks, which are probably due to standing waves on the shaft of the radial probe, move significantly as the density is changed. The perturbations are minimized as the shaft of the probe is moved behind the cutoff region where the pump field strength vanishes. Recently, new radial probes have been designed and installed with a U-shaped shaft; the portion of the shaft lying parallel to the electric field has been placed well behind the cutoff region, so that radial motion of the probe causes only a minimal perturbation of the electromagnetic wave.

III. INTERACTIONS OF MICROWAVES WITH PLASMA WAVES

1. Parametric Excitation of High Frequency Sidebands

As shown in Fig. 8, we observe near cutoff the excitation of high frequency oscillations visible as sidebands ($\omega = \omega_0 \pm n\Delta\omega$) of the pump line at ω_0, for pump powers above 2 to 3 watts. These results are very characteristic of the parametric decay instability in the following points: frequency matching is required, $\omega_0 \doteq \omega_{pe}$; there is a well defined pump threshold for excitation of the sidebands; the sideband spectrum is always asymmetric, favoring lower frequency oscillations, which rules out modulational effects; finally, the power in the sidebands saturates with increasing pump power. The results could be unequivocably attributed to the classic parametric decay instability if we could show a) that the sidebands have a wavelength appropriate to electrostatic Langmuir waves, and b) an ion acoustic wave with frequency equal to $\Delta\omega$ and wave number equal to the wave number of the electron wave. This work has not been completed yet, mainly because we have not been able to detect the corresponding ion wave in the presence of the low frequency noise. This low frequency noise could result from our method of detection which requires the probe to be biased positively to collect electron saturation current. A high-impedance probe designed to look at potential fluctuations could obviate this difficulty with low frequency noise.

The high frequency spectrum shows a variety of interesting decay processes, such as the one shown in Fig. 9, where multiple sidebands are excited with both harmonics and subharmonics. With increasing power these go over into a continuous, noisy lower sideband. In the ion frequency range we see essentially broadband noise. It is possible that the ion acoustic "partners" of the high frequency sideband are masked by this background noise. We have carefully studied the low frequency spectrum in order to find out whether this is the case or whether we are limited by inadequate receiver sensitivity, the probe bias or various other effects. The results are summarized in the next topic.

2. Excitation of Low Frequency Oscillations

We see pump-induced low frequency oscillations excited in four different cases: a) at high pump power ($\sim$ 15 W) with relatively high neutral

pressures, b) with floating probe bias, c) in the presence of two probes, and d) with two pumps.

a) At high pump powers, typically above 15 W, and relatively high neutral densities, typically above 1μ in pressure, enhancement of the low frequency noise occurs simultaneously with a high frequency spectrum which has a broad, noisy saturated character, as shown in Fig. 10. Both spectra increase and saturate at the same axial location and for the same matching conditions, $\omega_0 \doteq \omega_{pe}$. Thus there is strong evidence that this is a parametric decay, involving many waves in a broad spectrum rather than individual lines. We still have to establish that both low frequency noise and high frequency noise consists of waves. In general we can analyze the character of noise by using a two-probe spectral correlation technique: we filter a narrow frequency band out of the noise picked up on two independent probes, multiply the two signals and plot the time averaged product vs distance. Such a correlator is available with high sensitivity to analyze any low frequency noise up to 20 MHz. We have not done this measurement as yet because we did not have two probes present in the location of maximum noise enhancement. Another test to identify the source of noise consists of looking at the noise amplitude vs probe bias. At low load impedances (50Ω) noise density fluctuations due to ion waves appear dominantly above plasma potential. Figure 11 shows Langmuir probe traces with and without pump power. On the right hand trace one can see the enhanced noise above the plasma potential. There is no heating effect visible on the Langmuir probe traces, and the pump does not appear to modify the characteristic of the Langmuir probe in any other way. Thus this observed effect looks very much like a parametric decay instability and we are presently attempting to measure the wavelength.

b) Discrete lines in the ion spectrum corresponding to sidebands in the high frequency spectrum have been observed at negative, e.g., floating, probe potentials. This can be seen in Fig 12. Low frequency oscillations at $n\Delta\omega$ appear simultaneously with the high frequency sidebands, at $(\omega_0 \pm n\Delta\omega)$. However, for this probe bias we cannot detect grid-launched ion acoustic waves because of the strong effect of the plasma sheath surrounding the probe. It is believed that this low frequency oscillation is not a wave but a nonlinear mixing product between parametrically excited high frequency oscillation and the pump in the sheath.

c) Discrete lines in the low frequency spectrum are also seen when two probes biased at plasma potential are brought into close spacing, typically 2 to 3 cm (see Fig. 13). Again, an oscillation is excited above a certain pump power threshold and for frequency matching $\omega \doteq \omega_{pe}$. The ion oscillation is identified as a true ion acoustic wave with phase velocity near c_s velocity. But the amplitude of the line depends on the probe bias of the other probe and the probe spacing, and even on the presence of two probes. With a single probe we cannot detect the ion oscillation. It is possible that the probes excite beam plasma instabilities by drawing large electron saturation currents, typically 100 mA, and that the threshold of the instability is lowered by parametric pumping of the background plasma which decreases the ion wave damping.

d) With two pumps, ω_1, ω_2, near ω_{pe} we can excite density oscillation at the difference frequency $\Delta\omega = \omega_1 - \omega_2$. On the axial probe (see Fig. 14) we see with an interferometer set-up a large amplitude peak at the last pump standing wave peak before cutoff. No ion wave propagation in the axial direction has been observed to occur on the axis. The beat oscillation has, however, a distinctly different character when observed along the radial direction where the density gradient is much smaller than the axial direction (see Fig. 15). The wave is a density oscillation as our probe must be biased around the electron saturation region for optimum reception. The oscillation has a wave nature with wavelength decreasing in the radial direction. The wave propagates radially outward and the observed wavelengths near the center of the chamber are far too long to be normal ion acoustic modes. Since other ion oscillation peaks are seen at other large pump amplitudes, it is thought that nonlinear mechanisms other than parametric processes give rise to mixing and difference frequency signals, for instance, electron heating and temperature dependent collisions, i.e., the Luxembourg effect. However, heating must be very small since it is not seen on the Langmuir probe traces. Presently we have no satisfactory explanation for the change of wavelength and the fact that the phase velocity is so much higher than the sound velocity. In view of the fact that many nonlinearities can cause signals at the difference of two large electromagnetic waves, we have temporarily postponed the investigation of the two-pump case and will return to it after knowing more about the single pump parametric instability.

3. Ion Acoustic Wave Propagation in the Presence of an Electromagnetic Pump

Because of the difficulty in detecting parametrically excited ion acoustic waves which grow from noise levels, we have used a grid-launched test acoustic wave and observed the change in damping due to the pump. Figure 16 shows interferometer traces of launched ion acoustic waves at different densities in the presence of the microwave pump. The wave propagates parallel to the electric field, perpendicular to the density gradient. In a narrow range of densities, typically 2%, we see a modification of the ion acoustic wave propagation. At the optimum density, Fig. 17 shows the modification on an enlarged scale. With increasing pump power we can see a region of amplification in the ion acoustic wave propagation pattern. This is a strong evidence for a parametric modification of the background plasma. It is unlikely to be a probe effect, since the Langmuir probe characteristic is not changed by the electromagnetic wave. The probe is biased at plasma potential, that is, no sheath effects are present and no similar effects can be seen at other densities where the pump field at the probe tip can be even higher. If the pump power is raised to higher power levels (above 20 W) the parametrically excited broadband ion noise (see Fig. 10) damps the test wave, the amplification pattern becomes weaker and the traces become more noisy. Amplification is independent of the ion wave amplitude; at very low signals pumping brings the signal out of the background noise.

4. Mode Coupling of Electron Plasma Waves and Ion Acoustic Waves by an Electromagnetic Pump

Since the parametric process involves two plasma modes we have looked for excitation of electron plasma waves when propagating ion acoustic waves in the presence of the electromagnetic pump. Figure 18 shows that we observe sidebands of the pump at spacings equal to the ion acoustic wave frequency. The low frequency spectrum shows that launching large amplitude ion acoustic waves gives rise to harmonics, which explains the multiple sidebands in the high frequency spectrum. The sidebands in the high frequency spectrum are visible only in a narrow range of densities, typically 10% around optimum matching $\omega_0 = \omega_{pe}$. They are easily visible only below threshold of the parametric instability. Above threshold, the noise in the lower sideband of the high frequency spectrum (see Fig. 8) exceeds the amplitudes of the sidelines.

Since the sidebands are not seen on the magnetic loop antenna or on the scattered microwave pump signal, and since the amplitude depends on probe bias we have strong evidence that these sidebands are electrostatic waves. We have confirmed this fact by measuring the wave numbers of each individual line in a set-up shown in Fig. 19. Magnitude and direction of the k-vectors are measured by two channel phase lock-heterodyne receiver. The observed frequency spectrum around 2000 megacycles is frequency-converted with a local oscillator below the signal spectrum (this preserves the direction of the k-vector) to an intermediate frequency of typically 5 MHz where tuned high-Q RF amplifiers are available to filter out the individual lines. The reference frequency signal is created externally by mixing the small portion of the pump signal with the local oscillator, creating sidebands by an additional mixing with the ion frequency signal and filtering out the frequency component corresponding to the sideband frequency of interest. The direction of wave propagation is measured by observing the phase shift of a stationary phase point as the probe is moved. The magnitude of the wave number is measured by the conventional correlation technique.

Figure 20 shows both upper and lower first sidebands. The lower sideband is found to propagate opposite to the direction of the ion acoustic wave, with wave number approximately equal to the ion acoustic wave number. The upper sideband propagates parallel to the ion acoustic wave, also with wave numbers equal to the ion acoustic wave. The sidebands with spacing $n\omega_i$ have wave numbers nk_i and are due to mode coupling with the harmonics created by the large amplitude ion acoustic wave. All upper sidebands move with the ion wave, all lower sidebands opposite to it. Changing ω_i changes the wave number of the ion acoustic wave and thereby the wave number of the electron wave according to ion acoustic wave dispersion. Little amplitude dependence in the ion wave and the electron wave amplitude is observed as the ion wavelength is changed between 1.8 mm and 5 mm, corresponding to frequencies 350 MHz to 1 MHz. There appears to be no sharp distinction between the resonant and the slightly off-resonant mode for the electron plasma wave. A simultaneous comparison measurement between the three modes involved is shown in Fig. 21. The peculiar spatial behavior of the electron plasma wave may be related to the radial pump pattern and the small density gradient in the radial direction but nonnegligible density gradient.

Spatial behavior of the lower electron plasma wave sideband at different densities is shown in Fig. 22. The location for optimum mode coupling shifts to appreciable distances from the exciter grid as the density is lowered, which coincides with the radially outward shifting pump profile with decreasing density The spectrum also changes with probe position and density; near the grid the upper sidebands are favored; far away from the grid and at lower densities the lower sideband dominates. There is a relatively sharp decrease in the electron wave amplitude toward lower densities ($\omega_0 > \omega_{pe}$) which could result from heavy Landau damping. At small pump powers the electron wave amplitude is proportional to both the ion wave and the pump amplitude. For large pump amplitudes the parametrically excited noise fluctuations damp the coherent sidebands. There appears to be a transition from linear mode coupling to parametric mode coupling and to parametric instabilities.

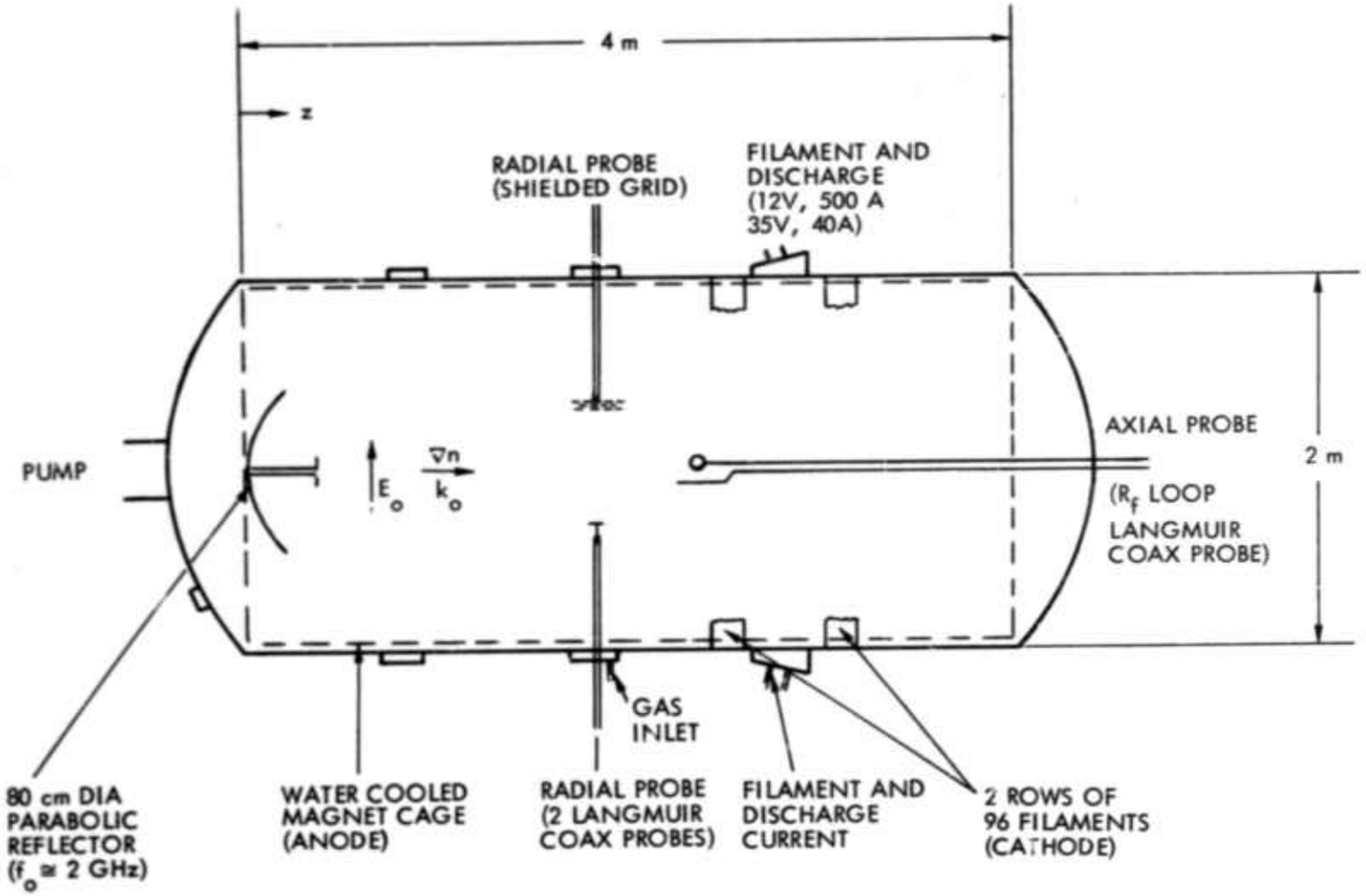

Figure 1. The QUIPS device

Table I - Typical Operating Characteristics

BASIC PLASMA PARAMETERS

(@ 1.3μ Argon, I_d = 41A, V_d = 35V)

Density	$n_e = 5.2 \times 10^{10}\ cm^{-3}$
Temperature	$kT_e = 1.6$ eV
Low Frequency Noise	$\delta n_e/n_e \lesssim 1\%$ $(0 < f < f_{pi} \simeq 7MHz)$
High Frequency Noise	$f \gtrsim f_{pe}$, $\Delta f \simeq 200$ MHz
Gradient Scale Length	$n/\nabla_z n \simeq 100$ cm
	$n/\nabla_r n > 500$ cm
Ambipolar Electric Field	$E_z \simeq 16$ mV/cm

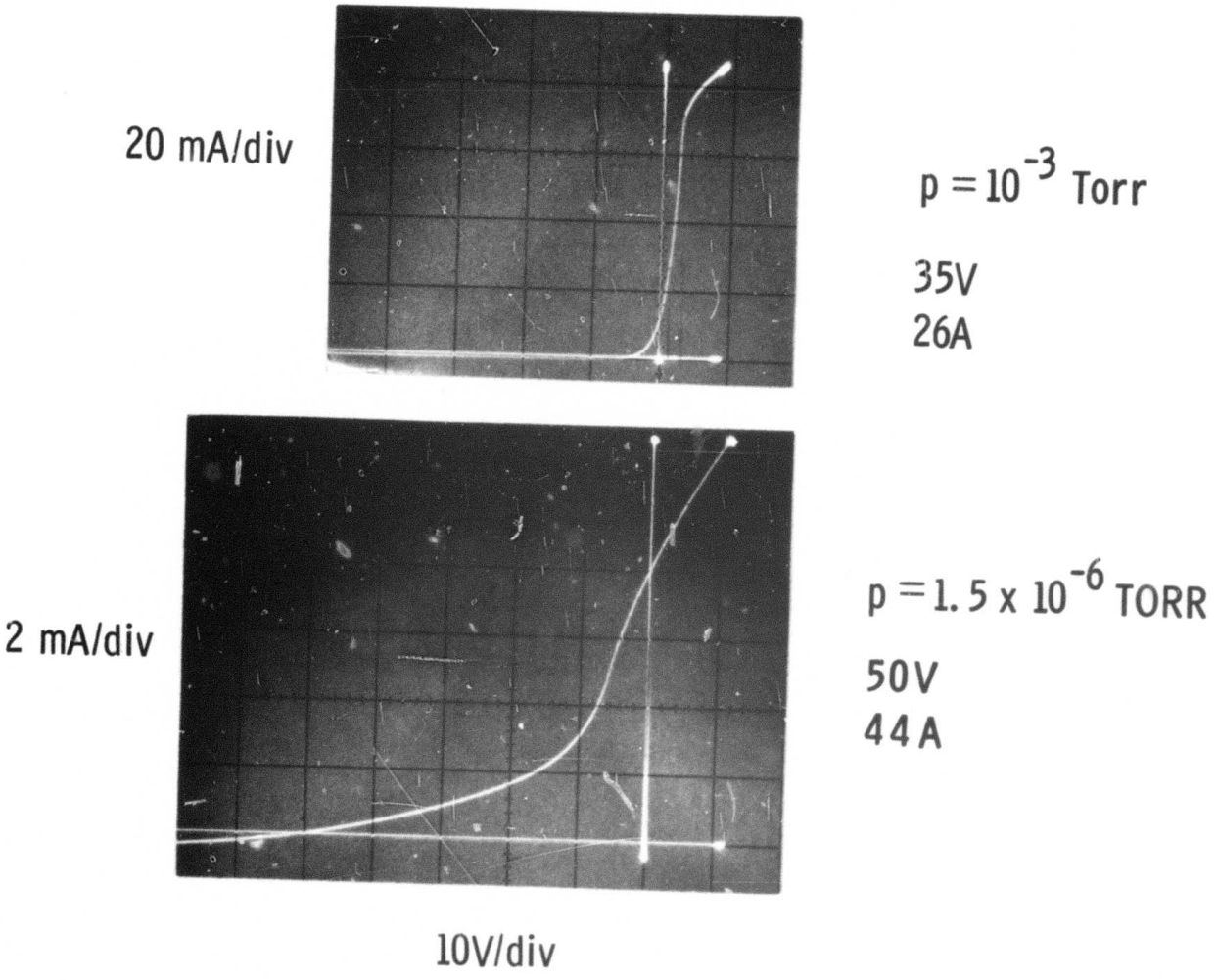

Figure 2 - Langmuir probe traces at high and low pressures

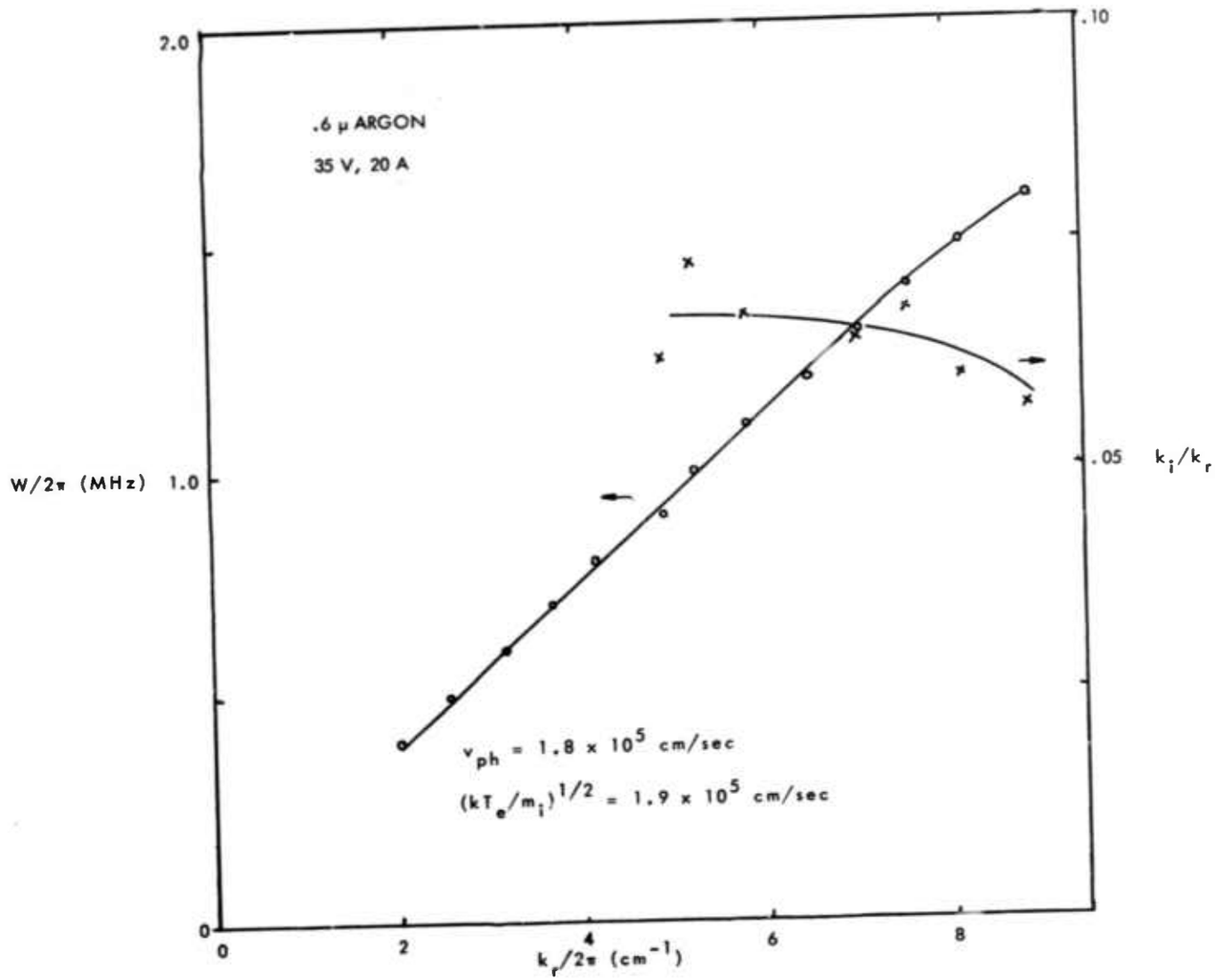

Figure 3 - Measured dispersion (0) and damping (x) of grid launched ion acoustic waves.

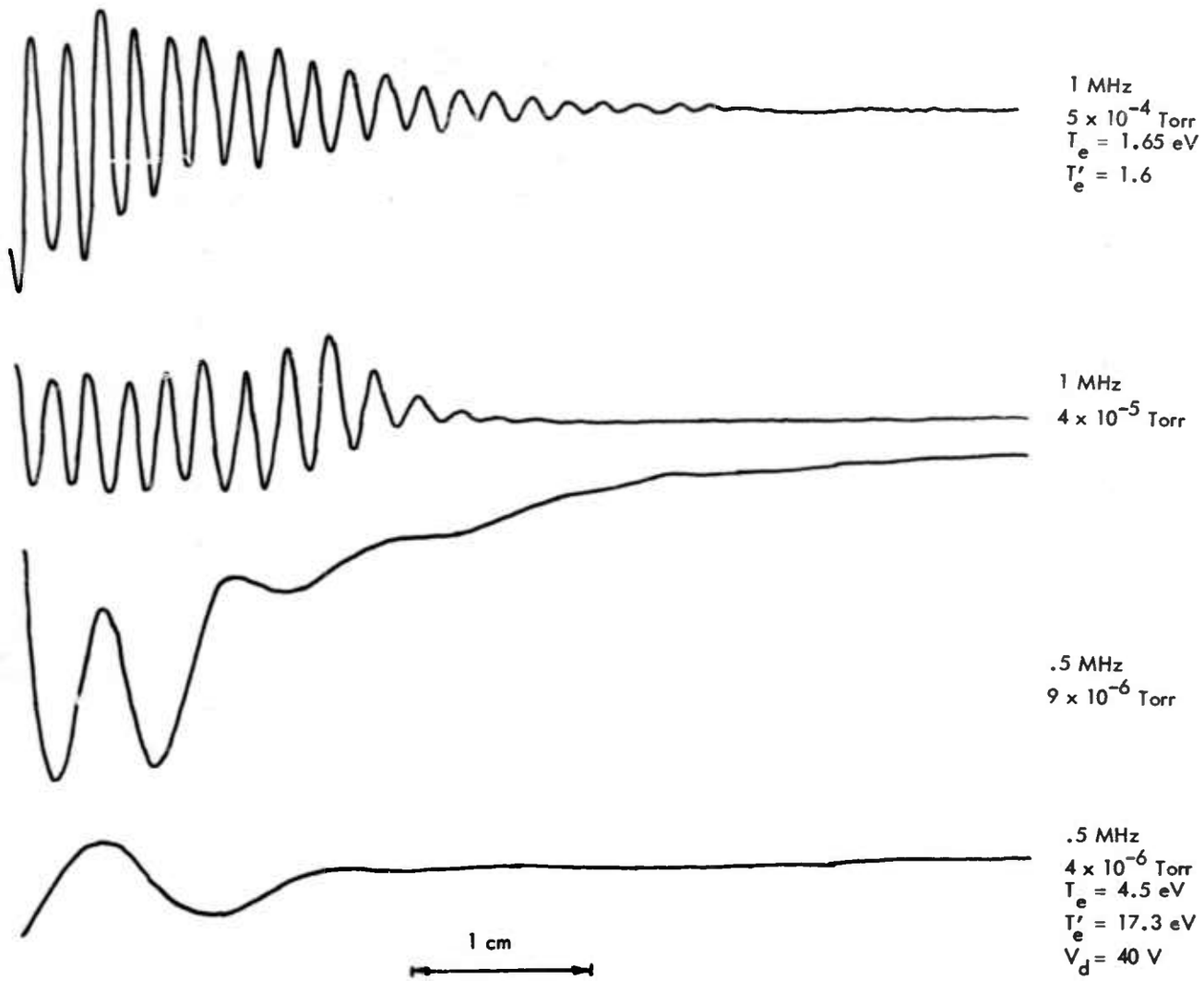

Figure 4 - Interferometer traces, for grid launched ion acoustic waves, at various pressures.

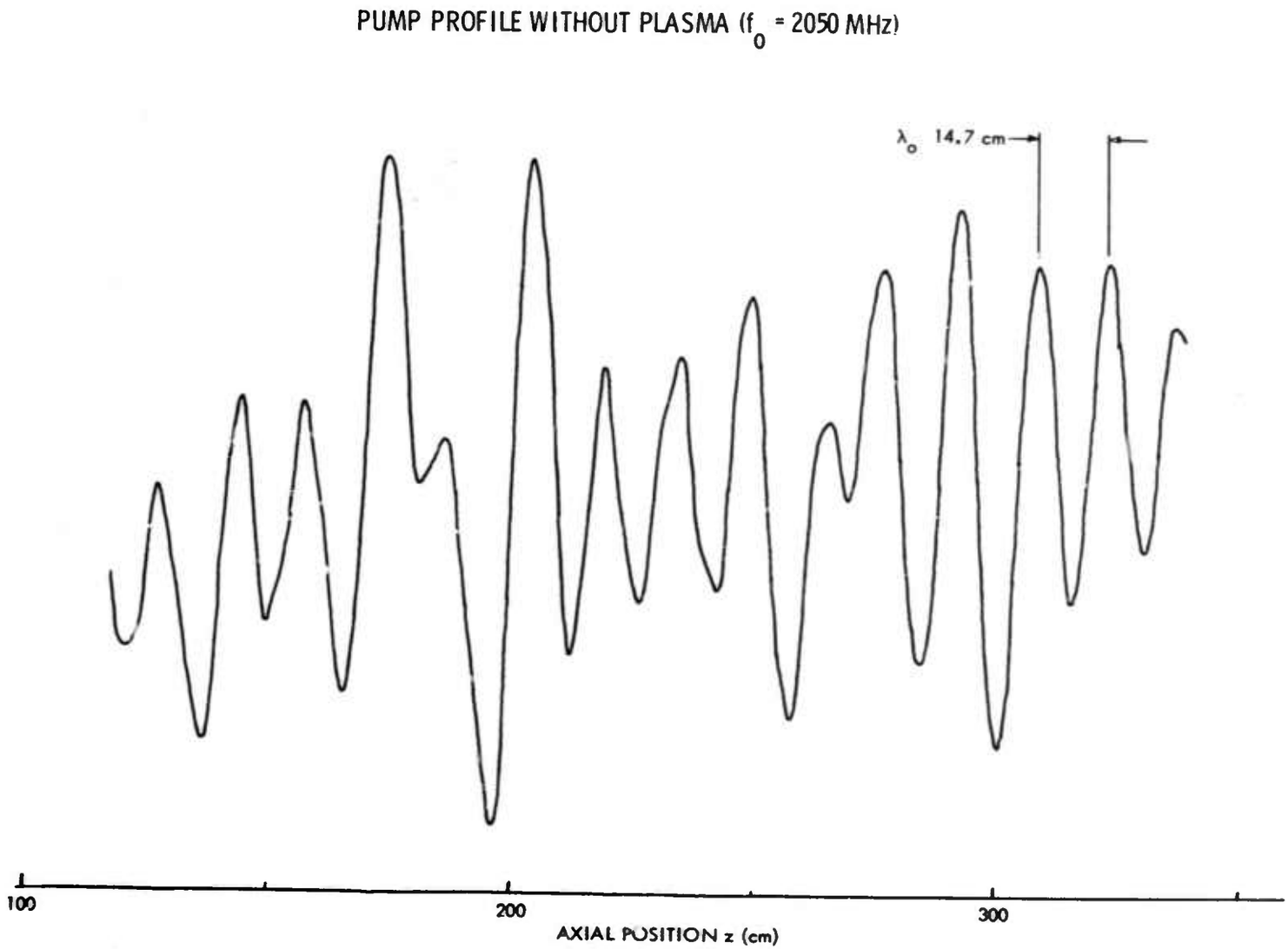

Figure 5 - Pump amplitude (arbitrary units) vs axial distance in the absence of plasma.

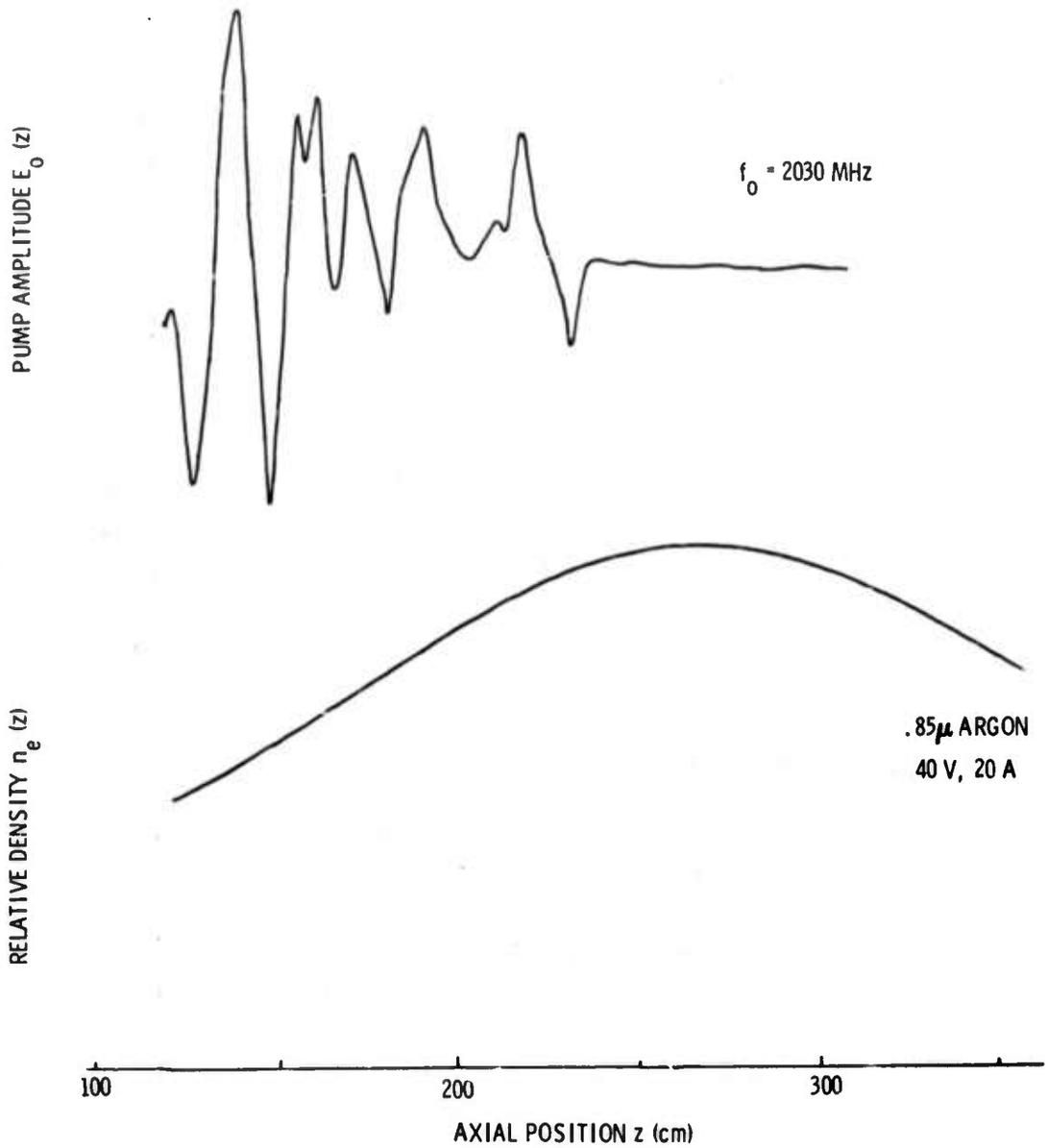

Figure 6 - Pump wave reflection, at the plasma cutoff, when propagating into a density gradient.

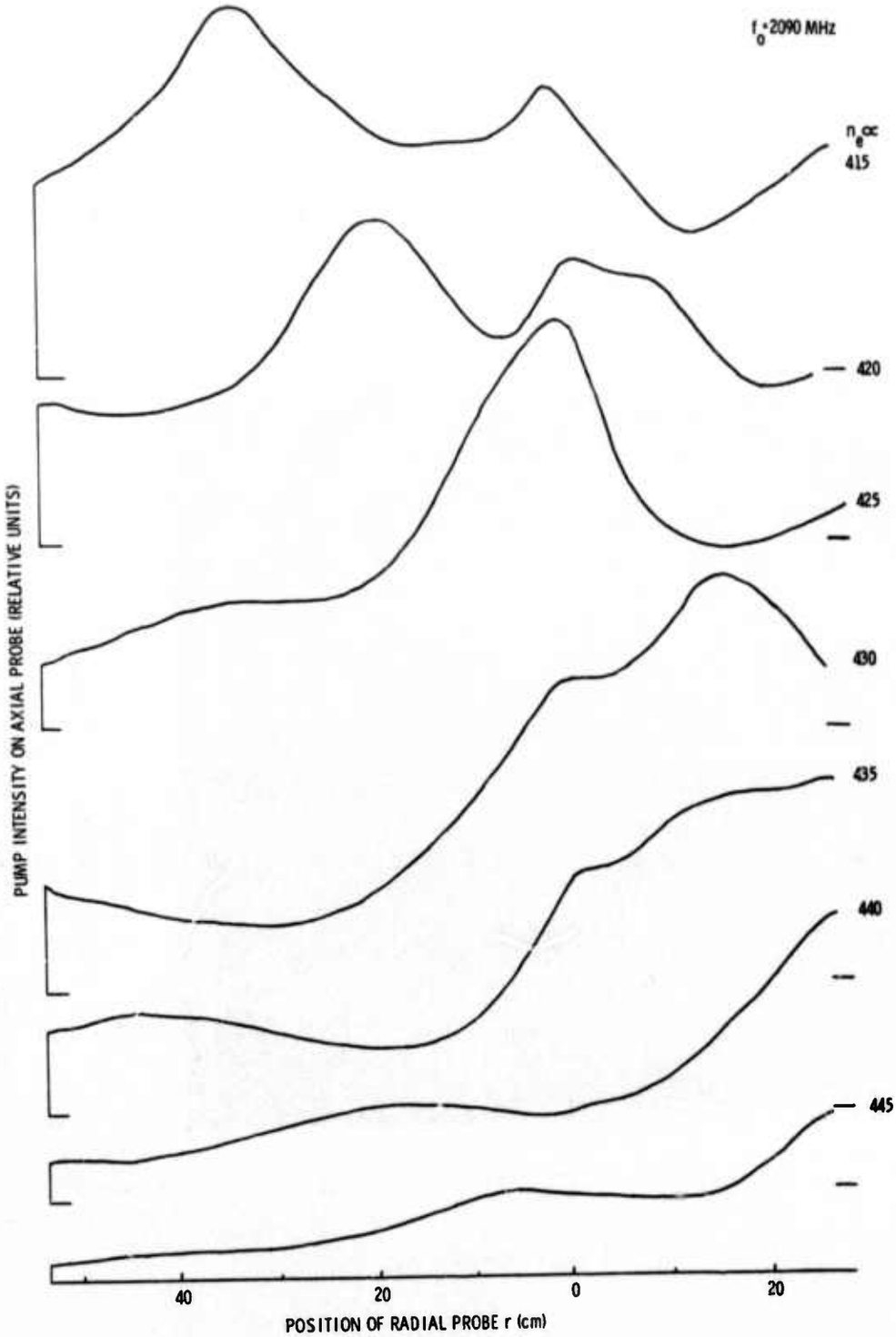

Figure 7 - Change of the pump pattern with radial probe position for various electron densities.

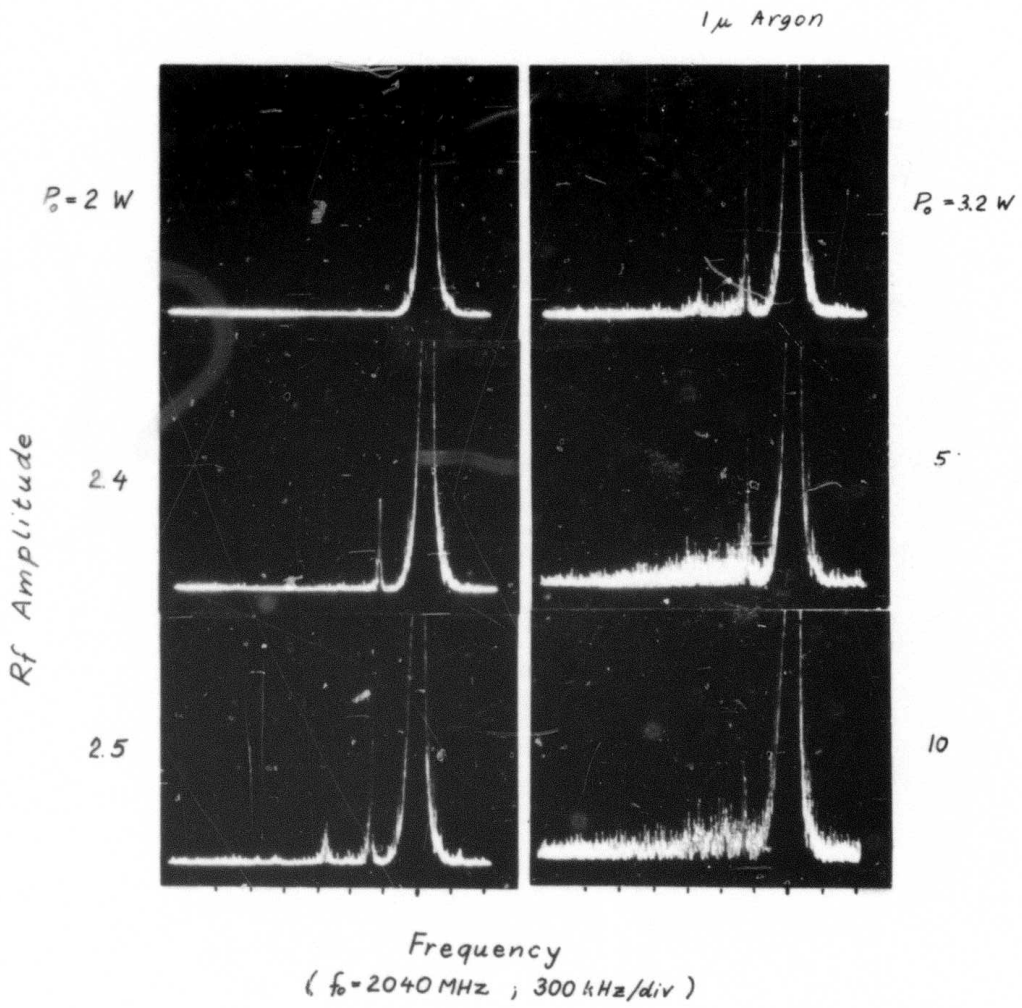

Figure 8 - Spectrum of plasma oscillations near the pump frequency, in the vicinity of the cutoff.

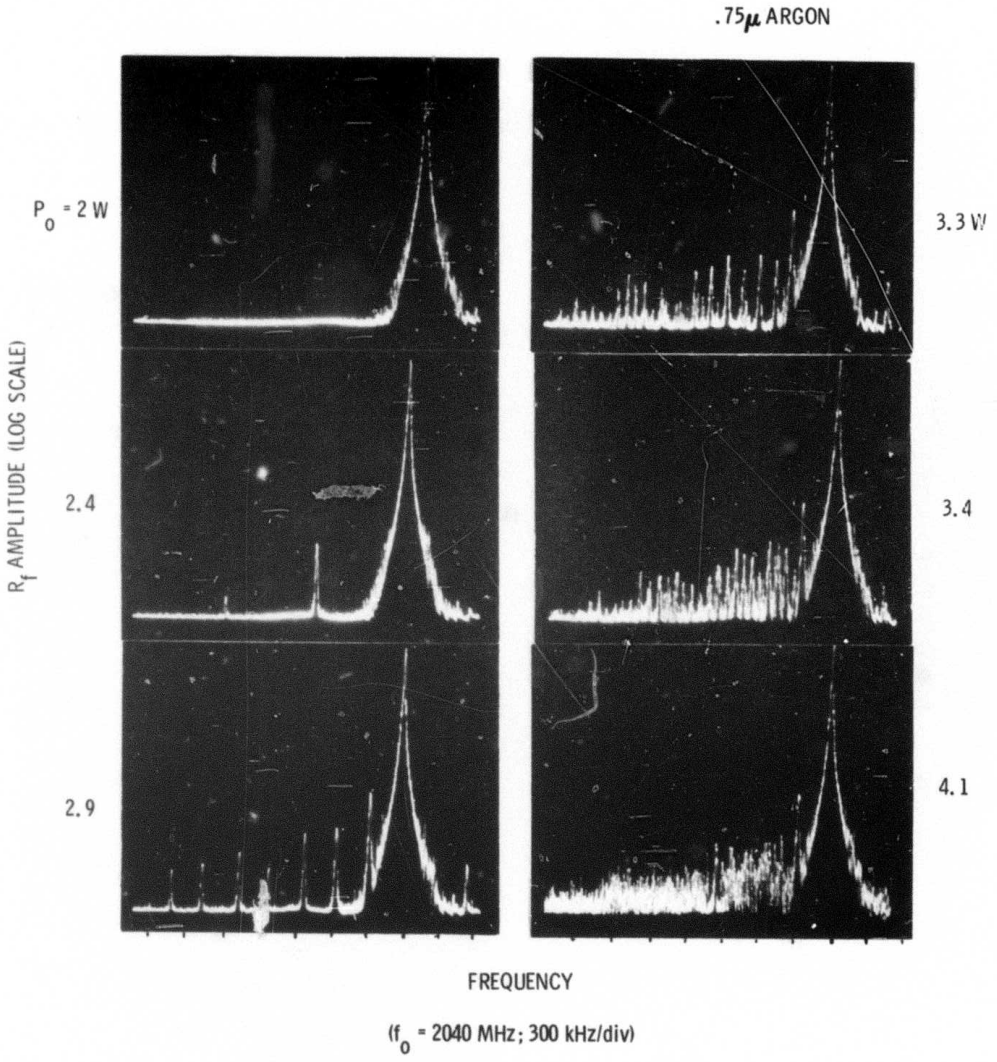

Figure 9 - Spectrum of plasma oscillations near the pump frequency, in the vicinity of the cutoff.

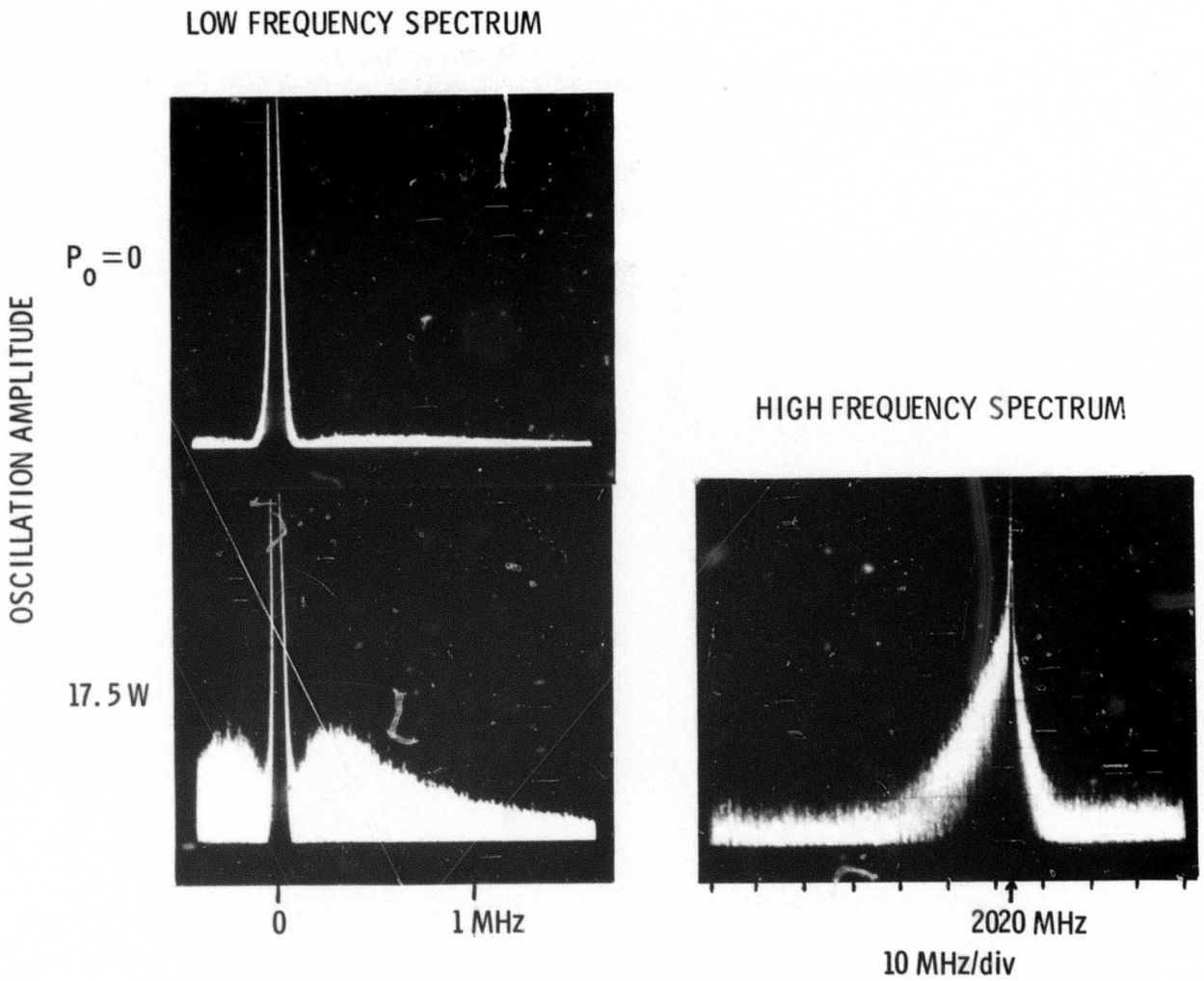

Figure 10 - Simultaneous enhancement of low and high frequency spectrum at high pump powers.

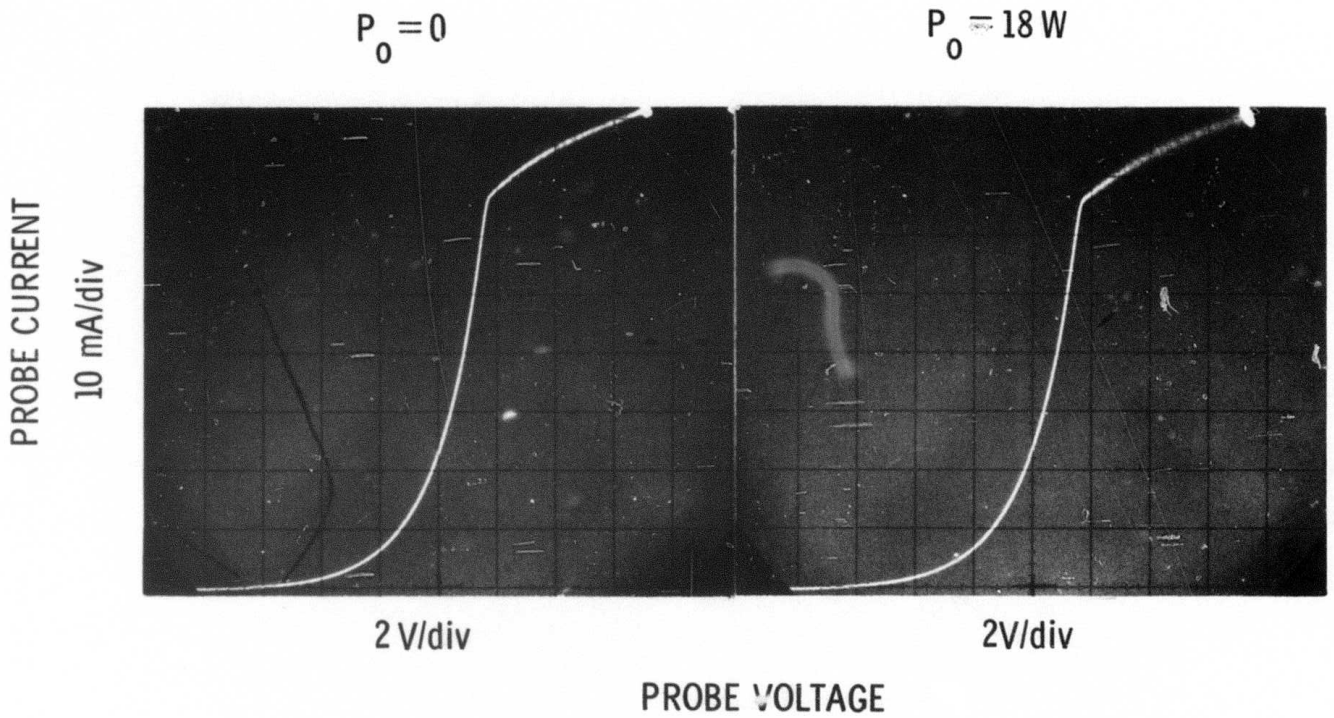

Figure 11 - Langmuir probe traces without and with pump power.

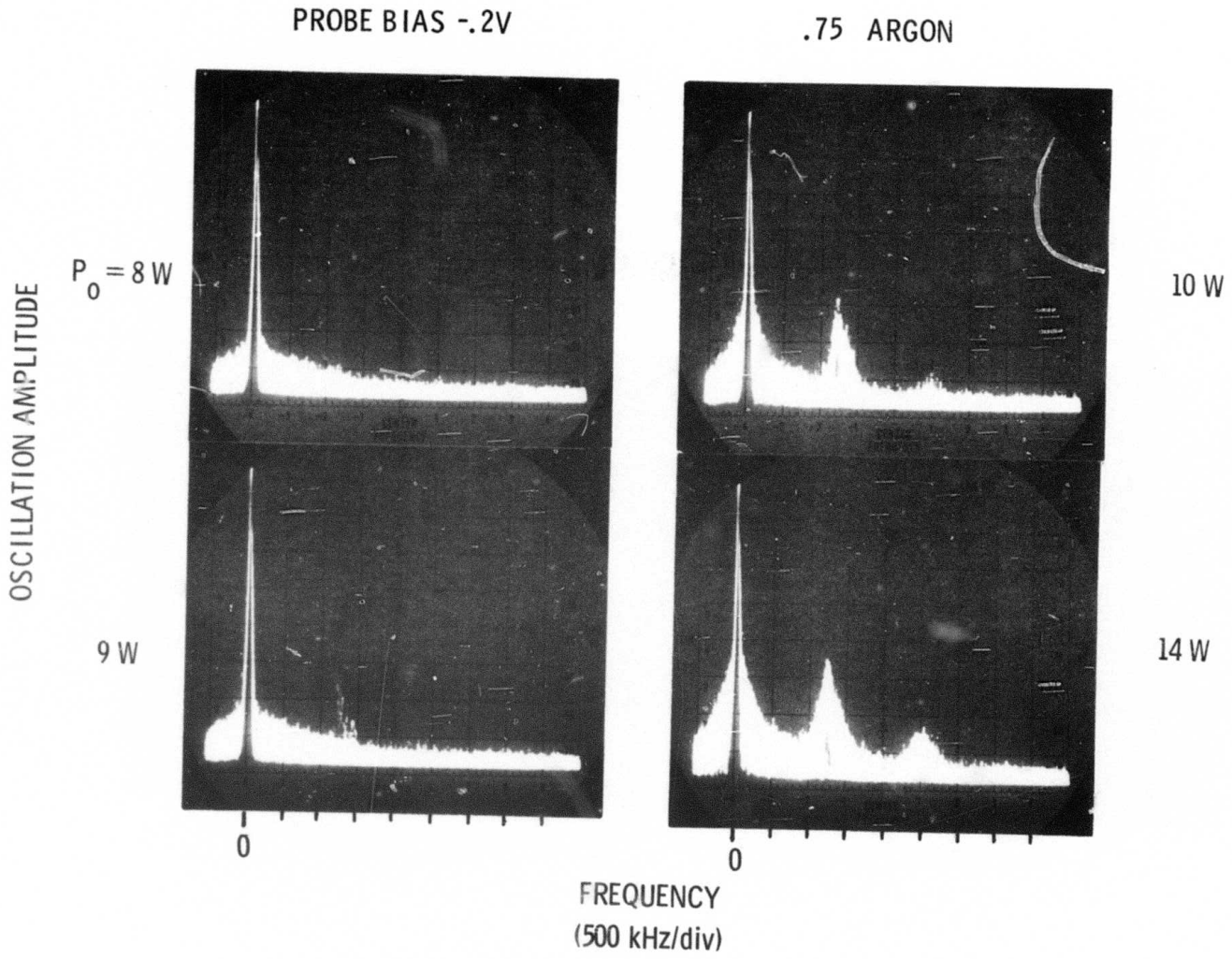

Figure 12 - Discrete lines in the ion spectrum corresponding to sidebands in the high frequency spectrum.

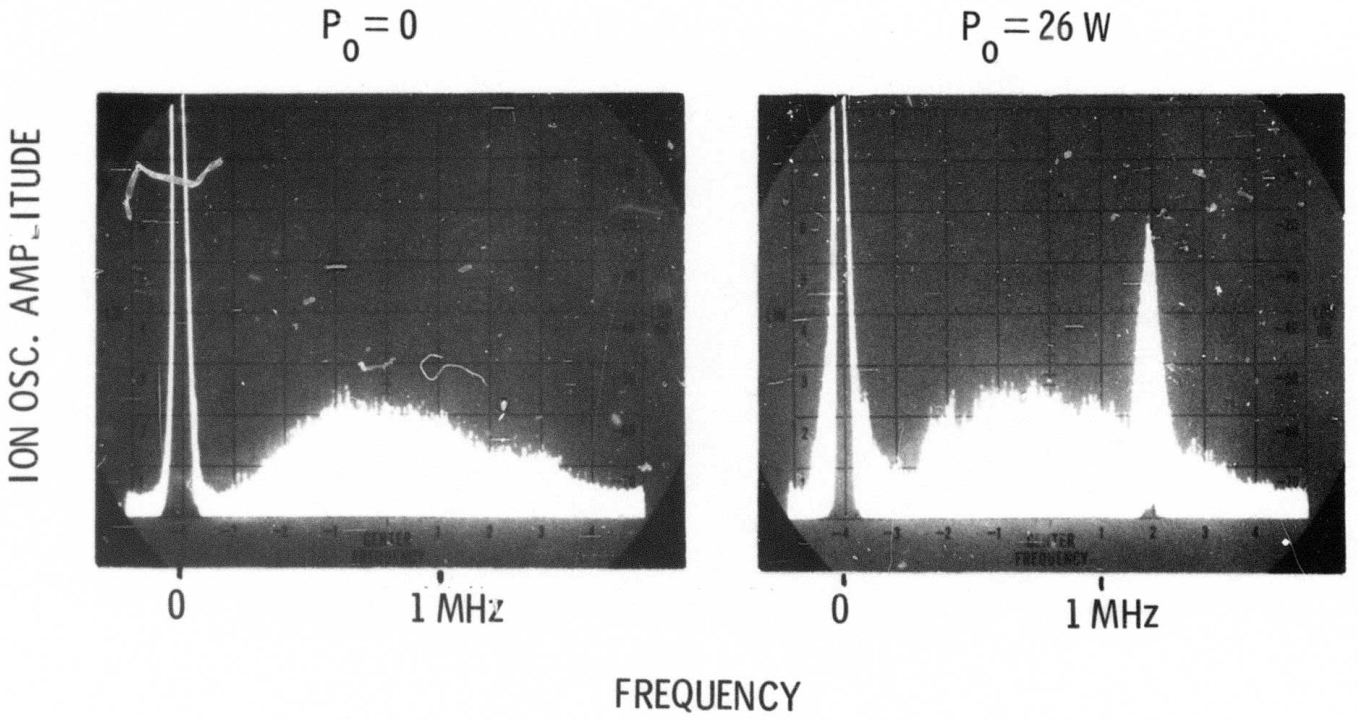

Figure 13 - Discrete lines in the ion spectrum in the presence of two closely spaced probes.

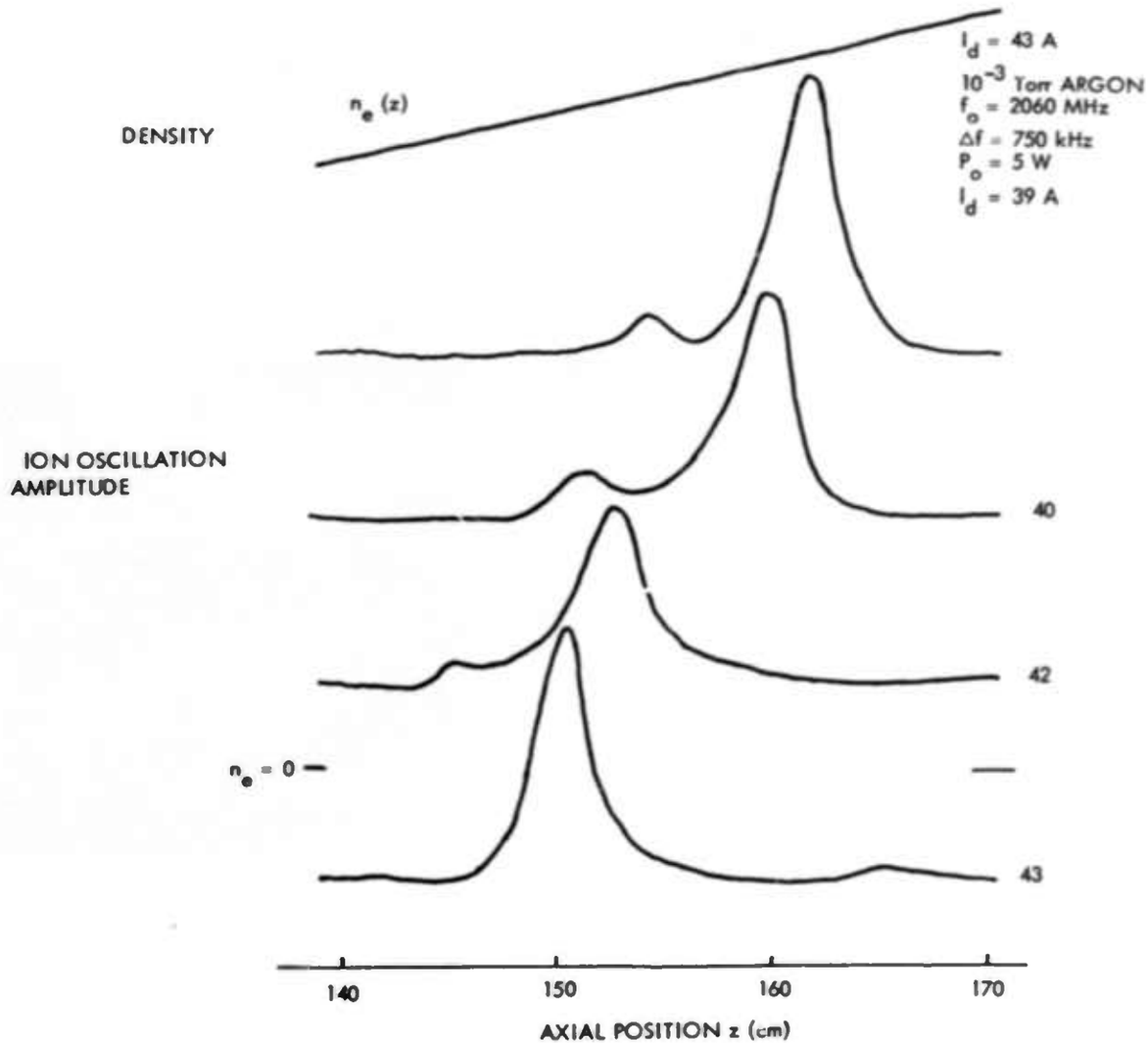

Figure 14 - Ion oscillations excited at the difference frequency, Δf, of two pumps for various maximum densities as seen with an interferometer on the axis.

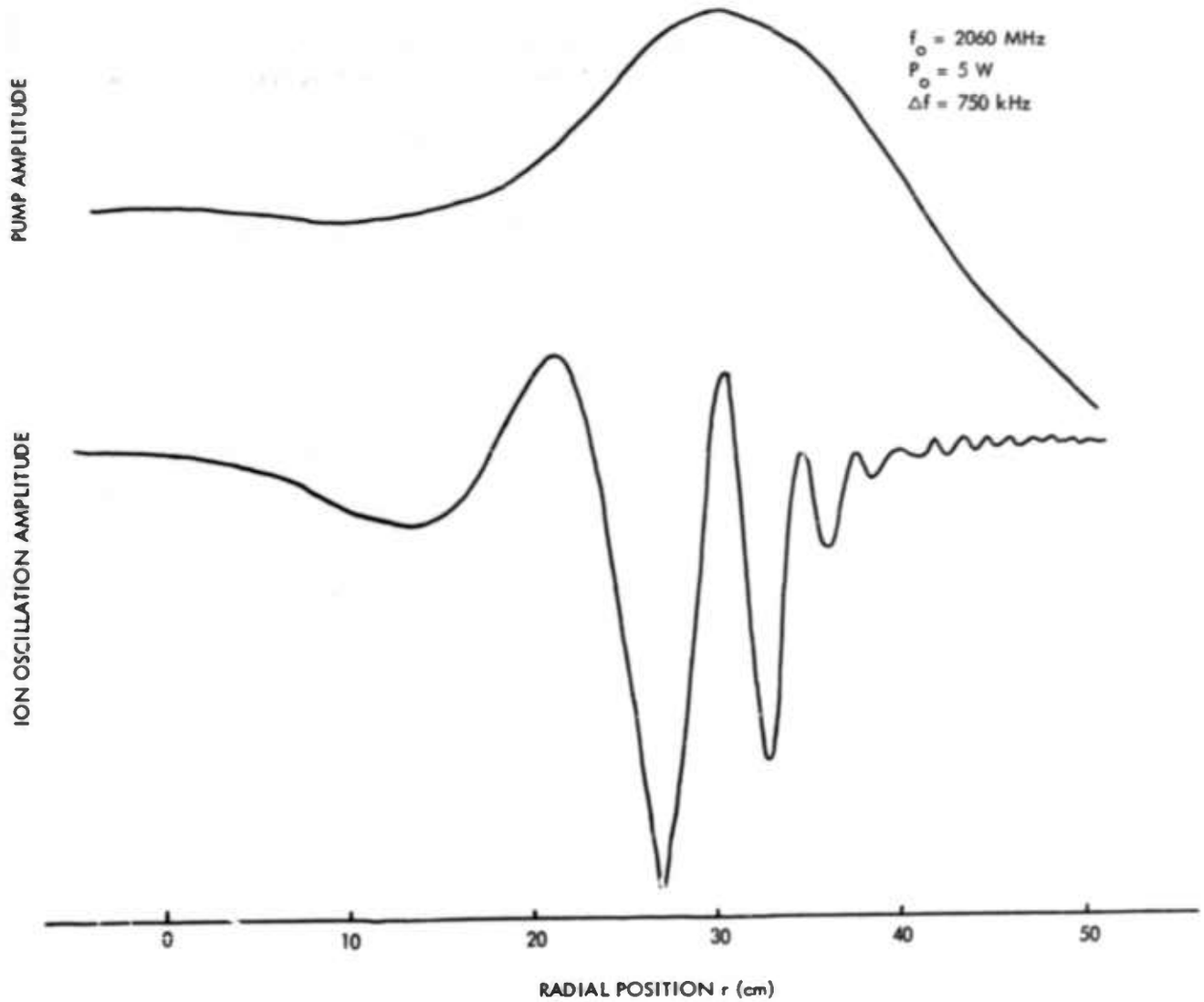

Figure 15 - Radially propagating ion oscillations excited by two pumps.

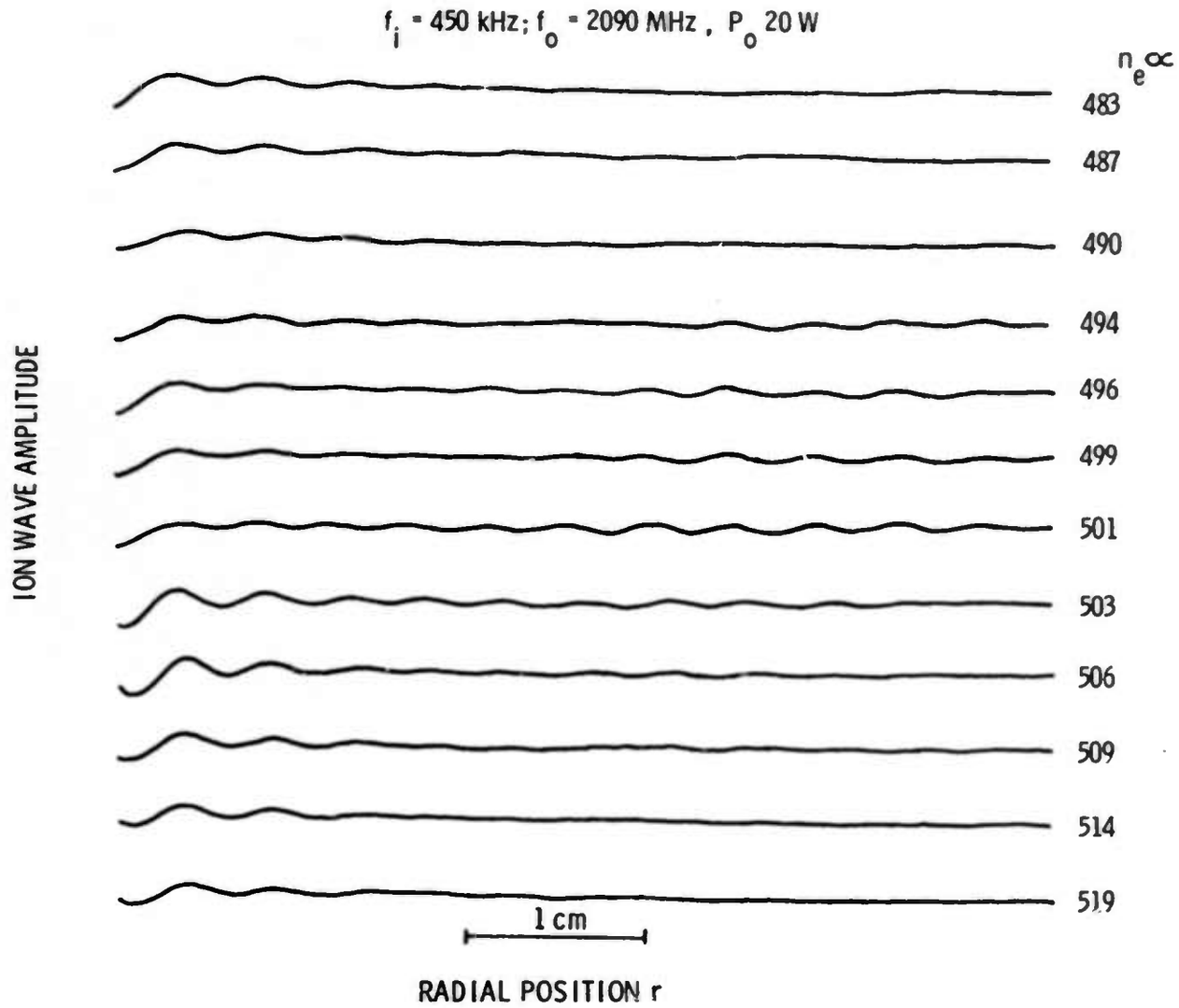

Figure 16 - Propagation of grid launched ion acoustic waves in the presence of the pump; at various plasma densities.

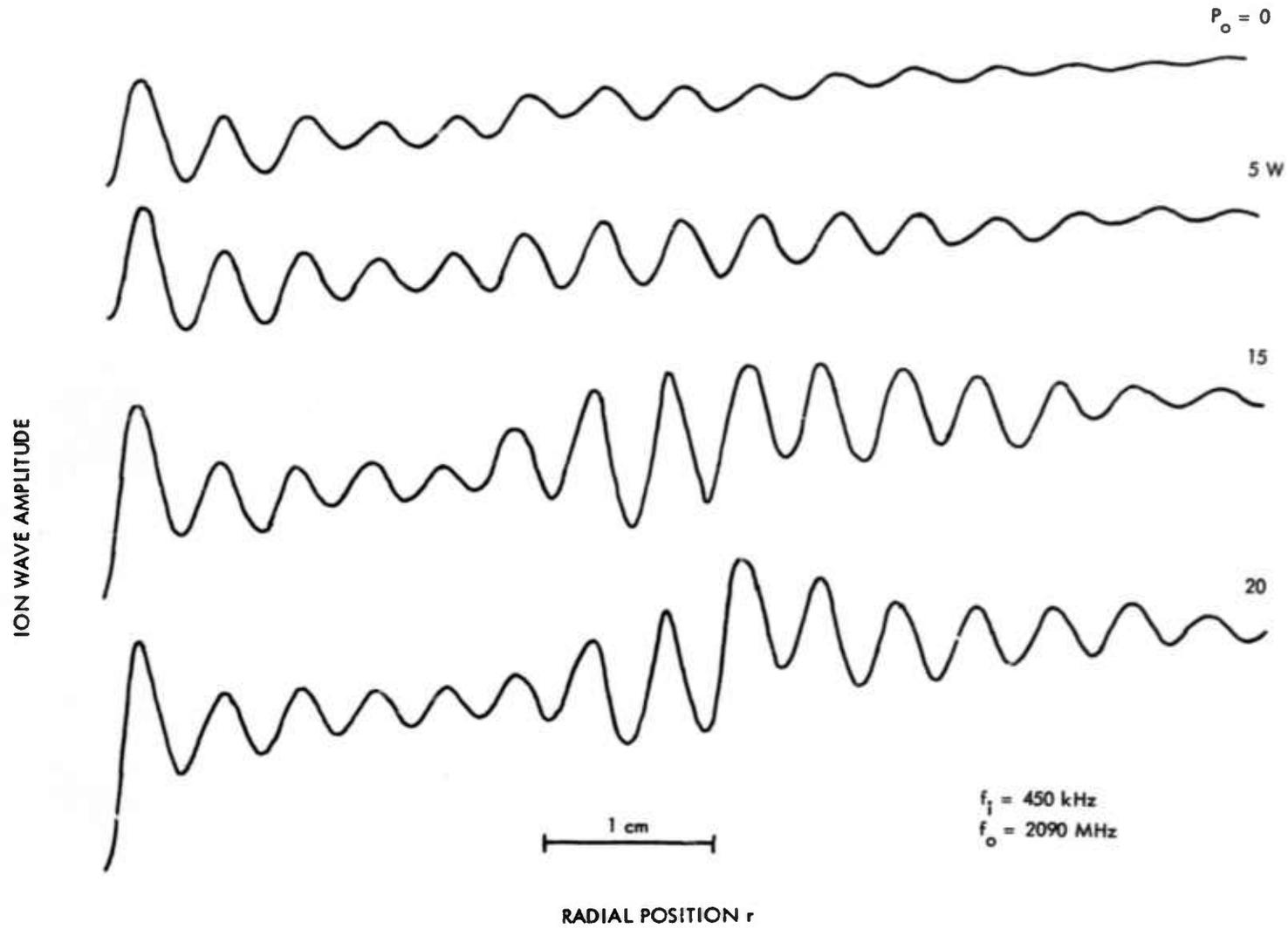

Figure 17 - Propagation of grid launched ion acoustic waves through the region of optimum density for various pump powers.

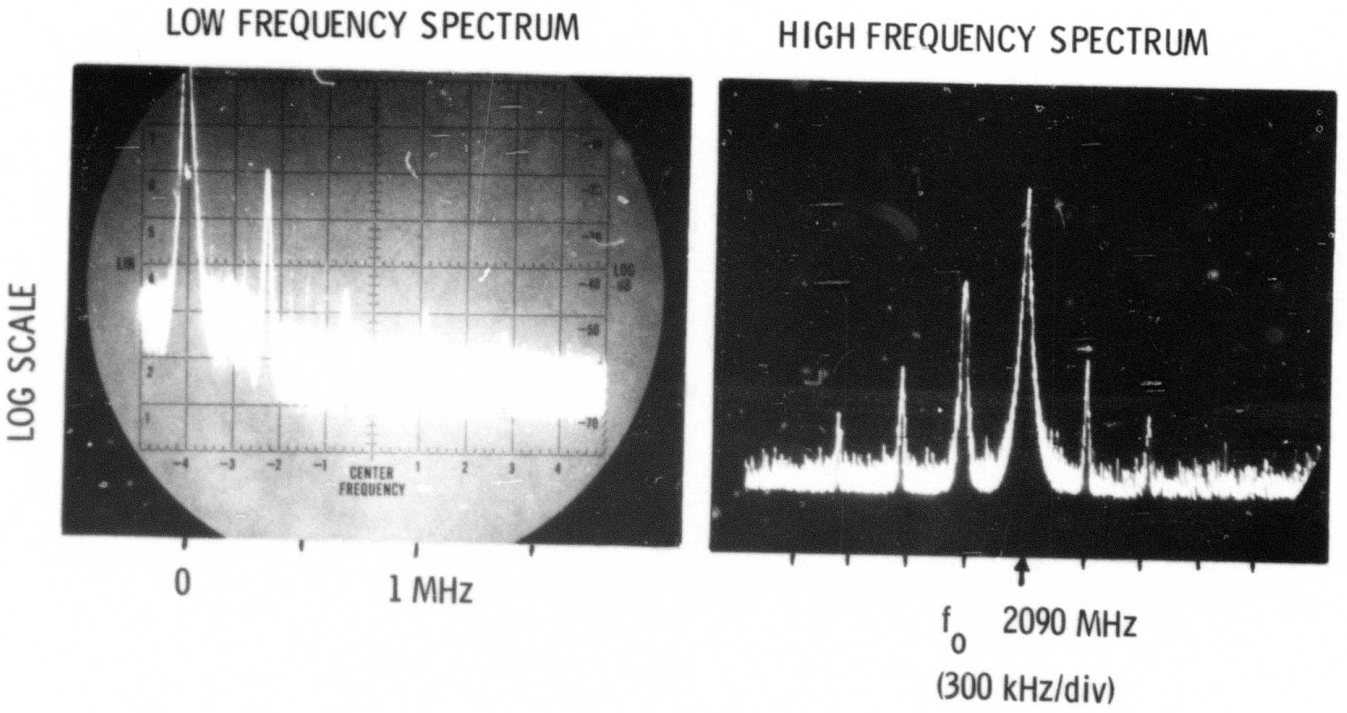

Figure 18 - Excitation of electron plasma waves when propagating ion acoustic waves in the presence of the pump. The pump is below the threshold for the parametric instability.

BLOCK DIAGRAM FOR k-VECTOR MEASUREMENTS OF ELECTRON PLASMA WAVE SIDEBANDS

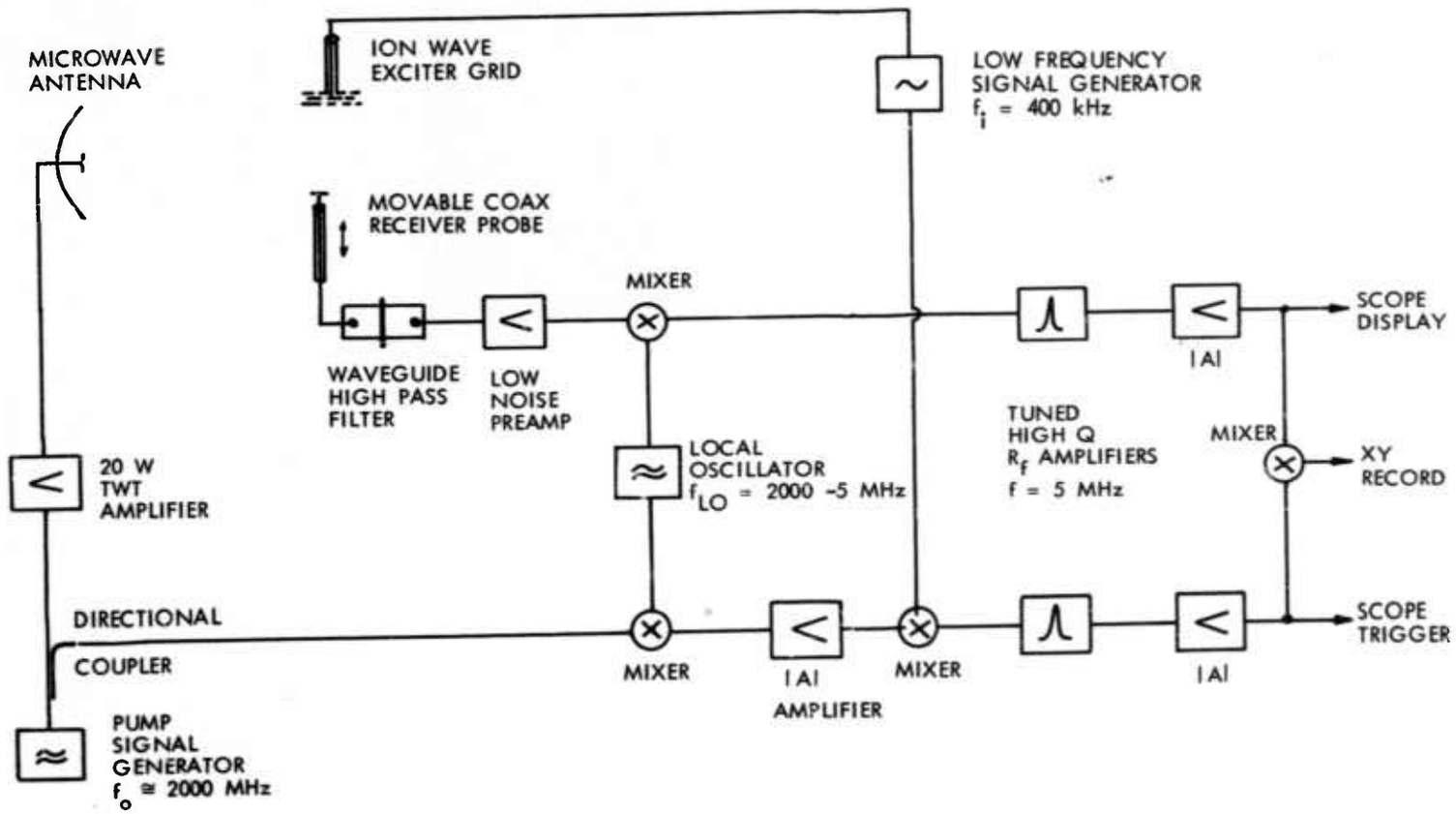

Figure 19 - Block diagram for k-vector measurements of electron plasma wave sidebands.

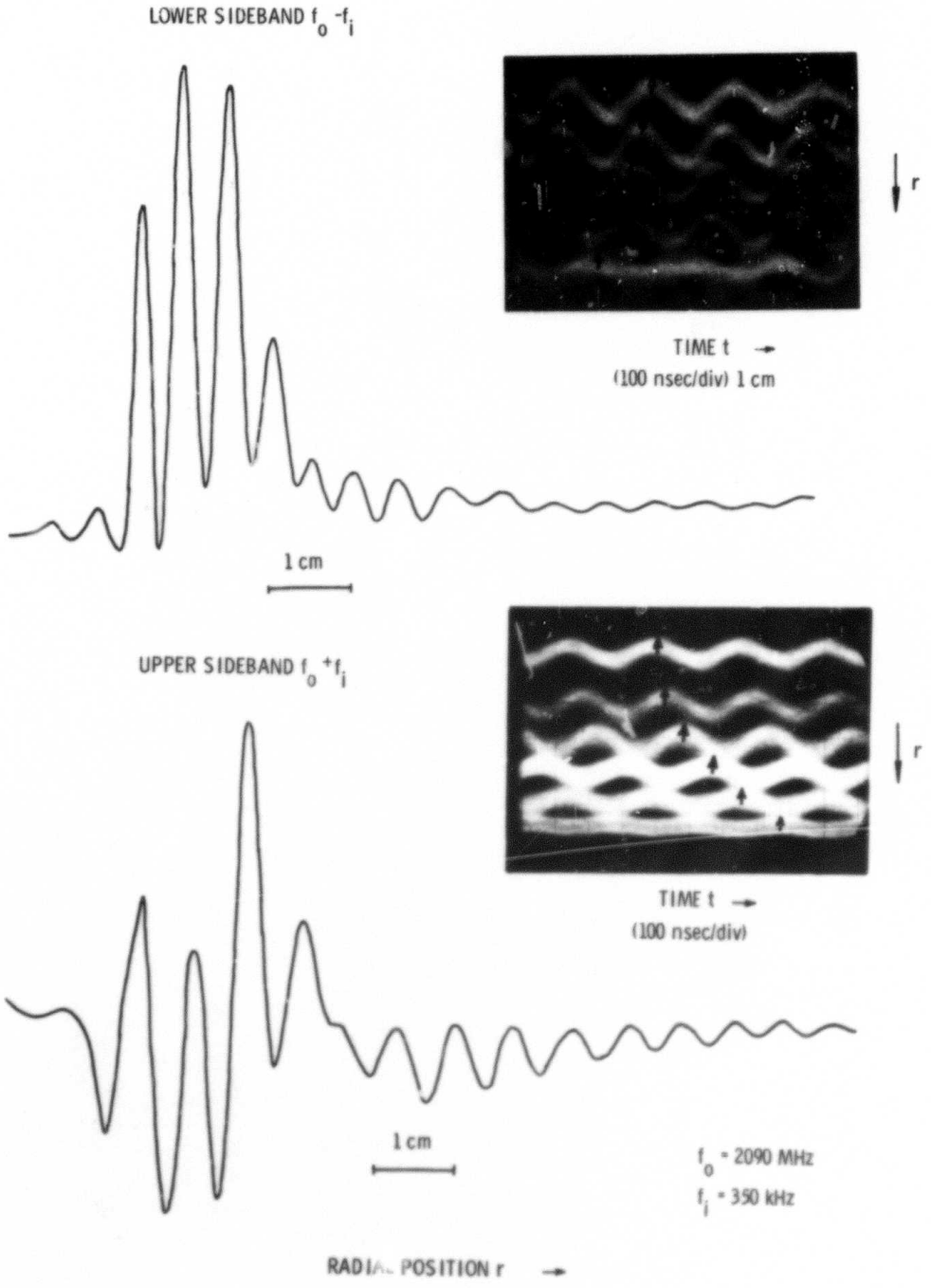

Figure 20 - Propagation of lower and upper electron plasma wave sidebands.

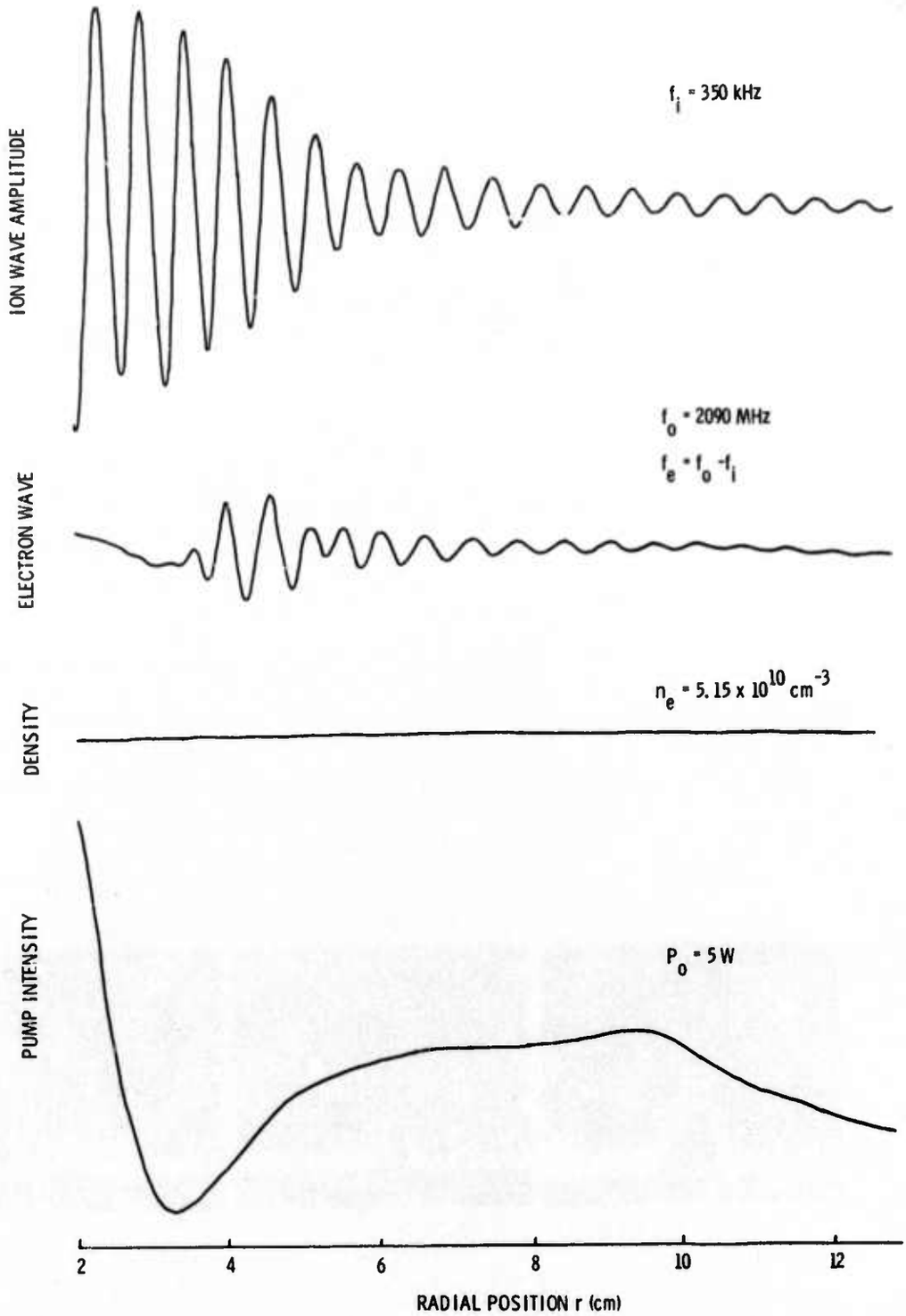

Figure 21 - Ion and electron wave amplitudes, plasma density and pump intensity vs radial position.

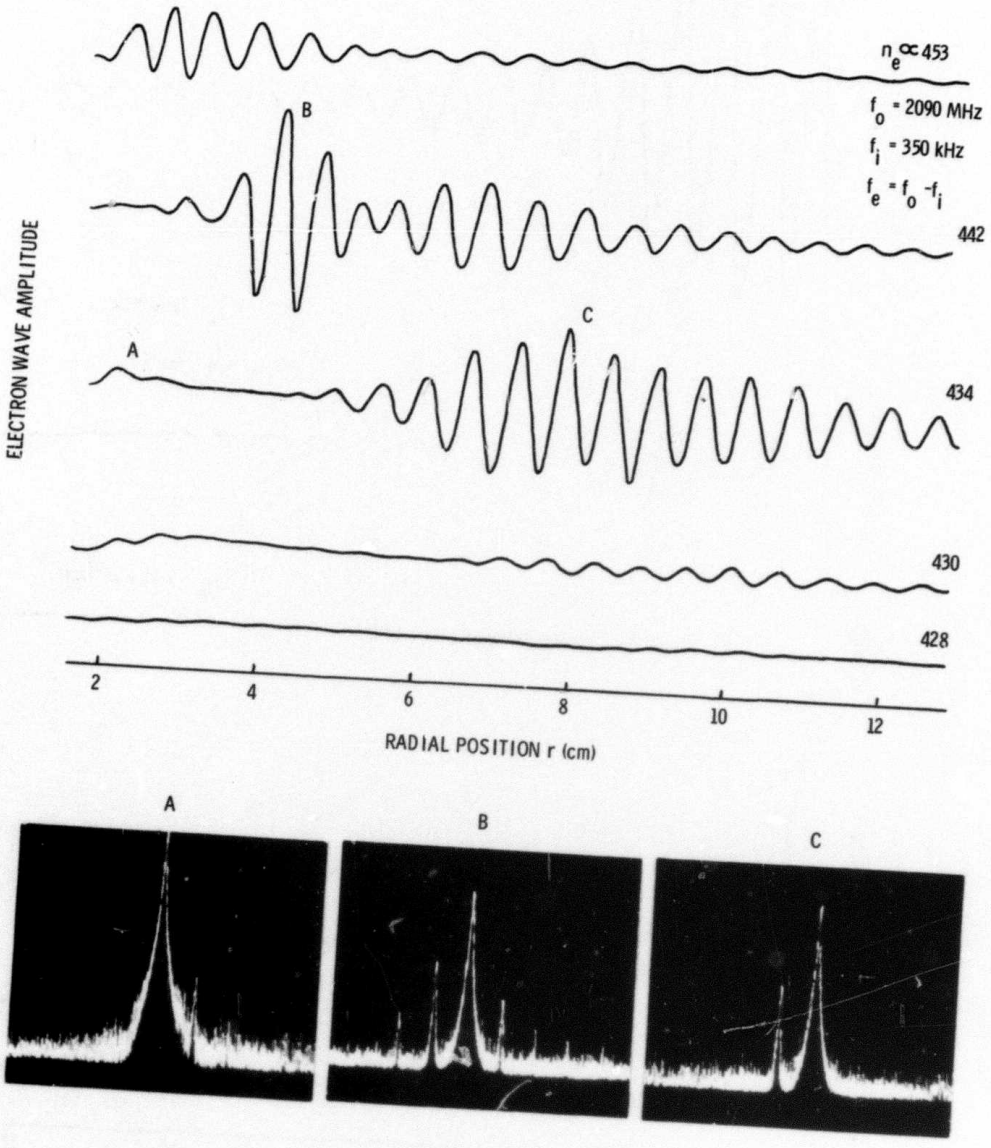

Figure 22 - Spatial dependence of the lower sideband at various plasma densities.